Energy Conversion and Management 300 (2024) 117916

Contents lists available at ScienceDirect

Energy Conversion and Management

journal homepage: www.elsevier.com/locate/enconman

Integration of power to gas and biomass charcoal in oxygen blast furnace ironmaking

Manuel Bailera [a,b,*], Boris Rebolledo [b]

[a] Escuela de Ingeniería y Arquitectura. Universidad de Zaragoza, Campus Río Ebro, María de Luna 3, 50018 Zaragoza, Spain
[b] Departamento de Ciencias Básicas, Facultad de Ciencias, Universidad del Bío-Bío, Chile

ARTICLE INFO

Keywords:
Ironmaking
Oxy-fuel
Biomass
Methanation

ABSTRACT

The paper introduces a novel approach for mitigating CO_2 emissions in blast furnaces by integrating top gas recycling, an oxy-fuel regime, power to gas, and biomass pyrolysis. Various case studies were conducted, involving the adjustment of pyrolysis temperatures (300 °C, 500 °C, 700 °C, and 900 °C) and varying the quantity of blast furnace gas directed to methanation for carbon recycling. Pinus radiata, abundant and cost-effective in Chile and Spain, was chosen as the biomass source. The integration was modeled using the extended operating line methodology and evaluated through 12 key performance indicators, such as flame temperature, coke consumption, CO_2 emissions, and specific primary energy consumption per unit of CO_2 avoided. Optimal performance was observed with pyrolysis at 700 °C and no blast furnace gas recycled through methanation. This configuration achieved a 58 % reduction in CO_2 emissions, with an energy consumption of 9.8 MJ/kg_{CO2}, and obviated the need for geological storage. Comparing this innovative proposal with other oxygen blast furnace approaches from the literature revealed a 13 percentage point improvement in CO_2 reduction over the second-best alternative. Additionally, the required electrolysis capacity, influencing capital expenditure, was 57 % lower, and energy consumption was reduced by 44 %.

1. Introduction

Iron and steel production are crucial for modern society, serving diverse applications in construction, transportation, and manufacturing. There are three primary routes for steel production: the blast furnace-basic oxygen furnace route (BF-BOF), the scrap-based electric arc furnace (Scrap-EAF), and the direct reduced iron-electric arc furnace (DRI-EAF).

The BF-BOF route stands as the predominant process in steel manufacturing, contributing to 70% of global production. It encompasses several key stages: the sinter strand, coke oven, blast furnace, basic oxygen furnace, and casting and rolling (see Fig. 1). Sintering is employed to agglomerate iron ore, while the coke oven facilitates the production of coke from coal. In the blast furnace, iron ore undergoes reduction by coke, yielding hot metal. Subsequently, the basic oxygen furnace reduces the carbon content of the molten iron to generate crude steel, which then undergoes casting and rolling to achieve the desired end product. Throughout these processes, various exhaust gases are generated and utilized as fuel within the integrated steel plant. This route is characterized by high energy and carbon intensity, resulting in a net energy consumption of 13–14 GJ/t_{HM} and specific emissions of 2,000 – 2,200 kg_{CO2}/t_{HM} [1].

The Scrap-EAF route involves the production of steel by melting recycled scrap using electricity. While it constitutes 23% of global steel production, its further expansion is constrained by the availability of scrap [1]. An alternative to this is the DRI-EAF route, wherein scrap is substituted with direct reduced iron, accounting for 7% of world steel production. Direct reduced iron contains over 90% metallic iron and is produced in combustion-free reactors that reduce iron ore using natural gas, hydrogen, or coal-based syngas [2]. The energy consumption for steel production through these routes varies from 4 to 10 GJ/t_{HM}, and the associated CO_2 emissions range between 300 and 1,300 kg_{CO2}/t_{HM}, depending on the proportion of scrap and DRI utilized [1].

The European Union's ambitious goal of reducing CO_2 emissions by 55% by 2030, with a further aim of achieving carbon neutrality by 2050 [3], has heightened interest in the development of low-emission technologies, particularly in industries responsible for 7% of global CO_2 emissions [4]. Despite this, the BF-BOF route is expected to maintain its dominance in the market as the global steel demand cannot be entirely met through recycled scrap. Furthermore, it is anticipated that at least 20% of current blast furnaces will still be in operation by 2050, as they

* Corresponding author at: Escuela de Ingeniería y Arquitectura. Universidad de Zaragoza, Campus Río Ebro, María de Luna 3, 50018 Zaragoza, Spain.
E-mail address: mbailera@unizar.es (M. Bailera).

https://doi.org/10.1016/j.enconman.2023.117916
Received 28 September 2023; Received in revised form 17 November 2023; Accepted 20 November 2023
Available online 28 November 2023
0196-8904/© 2023 The Authors. Published by Elsevier Ltd. This is an open access article under the CC BY-NC-ND license (http://creativecommons.org/licenses/by-nc-nd/4.0/).

Nomenclature

Acronyms and abbreviations

AFT	Adiabatic flame temperature
ASU	Air separation unit
BF	Blast furnace
BFG	Blast furnace gas
BOF	Basic oxygen furnace
BOFG	Basic oxygen furnace gas
CARB	Carburization
CC	Charcoal / Carbon capture
COG	Coke oven gas
daf	Dry ash free
DECOMP	Decomposition of coal
DIR	Direct
DRI	Direct reduced iron
EAF	Electric arc furnace
EX	Heat exchanger
HB	Hot blast
HHV	Higher heating value
HL	Heat loss
HM	Hot metal
INJ / J	Injection
IR	Iron
KPI	Key performance indicator
M	Mid
OBF	Oxygen blast furnace
OR	Ore
PCI	Pulverized coal injection
PtG	Power to Gas
RED	Reduction
RG	Reducing gas
SNG	Synthetic natural gas
SPECCA	Specific primary energy consumption per unit of CO_2 avoided
TGR	Top gas recycling
U	Upper

Symbols

M	Molar weight, kg/kmol
n	Mole flow, mol/t_{HM}
Y	Yield ratio (mass basis), -

Subscripts and superscripts

B	Biomass
BFG	Blast furnace gas
CC	Charcoal
i	Component i
SYN	Syngas

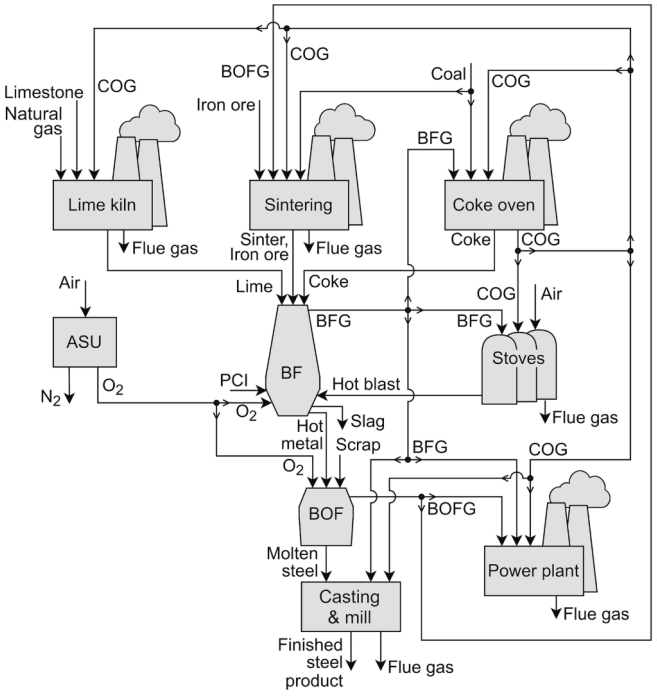

Fig. 1. Typical process flow diagram of an integrated BF-BOF steel-making plant.

are typically phased out during relining, a process that occurs every 20 to 40 years [5]. Consequently, there is a pressing need to innovate and develop methods for reducing CO_2 emissions in blast furnaces.

2. Literature review

One approach for reducing CO_2 emissions in blast furnaces is top gas recycling (TGR), involving the recycling of the blast furnace's exhaust gas back into the process. This recycled gas serves as a reducing agent to decrease coke consumption (Fig. 2). The typical composition of this gas is approximately 22% – 24% CO_2, 20% – 25% CO, 0% – 2% H_2O, 3% – 4% H_2, and 47% – 53% N_2, by volume. However, injecting CO_2 or H_2O directly into the blast furnace is undesirable, as it can increase fuel consumption and impede the reduction of iron oxides by disrupting the chemical equilibrium. To address this, a carbon capture stage is often incorporated before recycling the top gas, allowing for the removal of 90% to 100% of the CO_2 [6–11]. The recirculated gas can be introduced at various points, such as the tuyeres, the shaft, the preparation zone, or a combination of these locations [4]. The CO_2 reduction achieved by this method is limited to approximately 15% due to the presence of N_2 in the recirculated gas [12].

The top gas recycling technique, initially designed to valorize an exhaust gas, shares similarities with oxy-fuel combustion processes. In both cases, a gas stream is recirculated, and a carbon capture stage is essential. Consequently, top gas recycling has evolved to the possibility of integrating it with oxygen blast furnaces (OBF) (Fig. 2). Oxygen blast furnaces utilize pure oxygen instead of air for coke combustion, reducing the need for fossil fuel and improving energy efficiency. As a portion of the blast furnace gas is recirculated in top gas recycling, it addresses the nitrogen deficiency during oxy-fuel combustion, maintaining similar fluid and thermodynamic behavior to air-blown combustion. This enables a reduction in coke consumption by 14 – 150 kg/t_{HM} (a 5% – 34% decrease compared to conventional BF) [4]. Prototype-scale oxygen blast furnaces have demonstrated a minimum feasible coke rate of 200 – 230 kg/t_{HM} [13]. The associated decrease in CO_2 emissions falls within the range of 100 to 500 kg_{CO2}/t_{HM}, translating to a 10% – 40% reduction compared to conventional BF [6,14–20]. Additionally, as CO_2 is extracted from the recycled top gas through a capture stage during recycling, a substantial amount of highly-concentrated CO_2 gas becomes available for underground storage [4].

An alternative approach to leverage captured CO_2 involves combining oxygen blast furnaces with Power to Gas (PtG) technology (Fig. 2) [21]. PtG technology utilizes renewable electricity for water electrolysis, producing H_2, which is then combined with CO_2 emissions from the ironmaking process to generate synthetic natural gas (SNG)

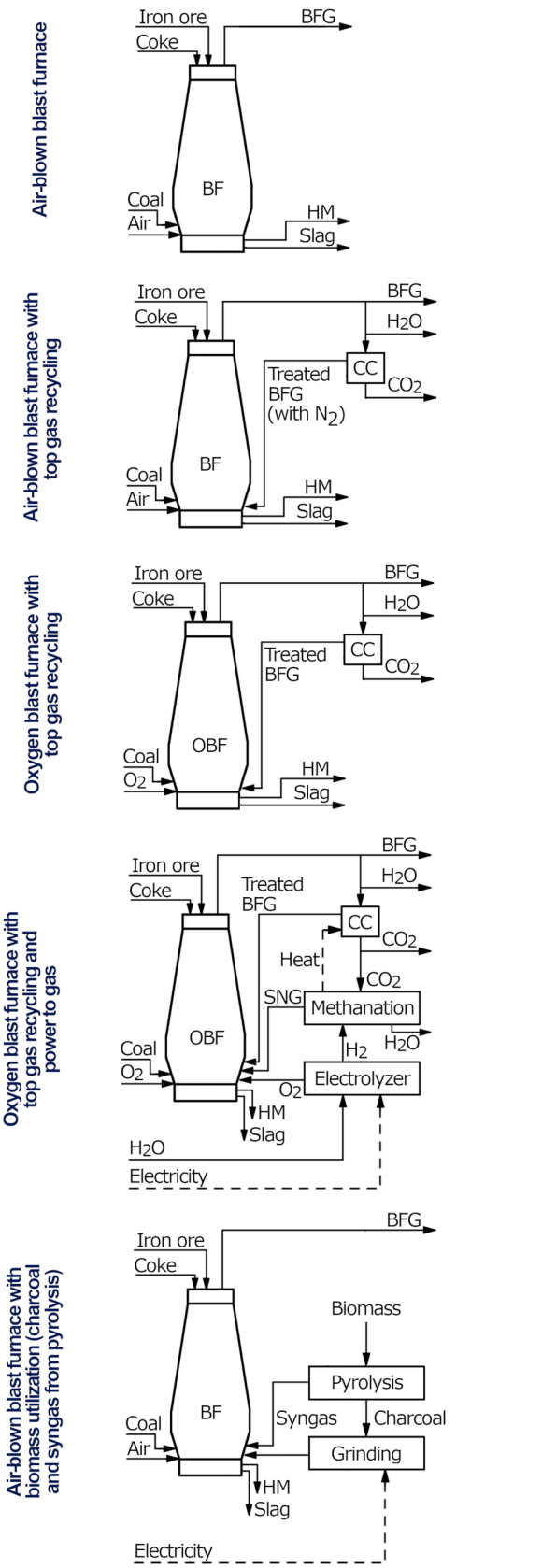

Fig. 2. Process flow diagram of conventional blast furnace (air-blown) and its modifications for reducing CO_2 emissions.

[22,23]. This synthetic fuel is employed in the blast furnace, establishing a closed loop for carbon and obviating the need for geological storage [24,25]. Approximately 70 – 90 kg/t_{HM} of CO_2 can be maintained in a closed loop, preventing permanent storage, and accounting for 5% – 7% of emissions from a conventional BF. Consequently, the integration of OBF with PtG could potentially reduce emissions by around 45% compared to air-blown blast furnaces. Additionally, the electrolysis process in PtG produces O_2, which can be utilized in the oxygen blast furnace, thereby reducing the electricity consumption of the air separation unit needed to enrich the hot blast in OBF [26,27]. Depending on the technological advancement of the steel plant, the consumption of the air separation unit may range from 260 to 400 kWh/t_{O2} [16,28].

Other strategy for CO_2 reduction in blast furnaces involves the utilization of biomass resources. Without any pre-treatment, biomass could only serve as a substitute for the pulverized coal injected at the tuyeres. However, the poor grindability of raw biomass results in excessive energy requirements for grinding. Moreover, its low energy density necessitates a larger quantity of biomass compared to coal, leading to increased ash content in the blast furnace and causing operational challenges [29]. A common approach for incorporating biomass in ironmaking is the production of charcoal, the solid product obtained through the torrefaction or pyrolysis of biomass. This process upgrades biomass for ironmaking, achieving comparable heating values and similar O/C and H/C ratios to coal. Nevertheless, the low mechanical strength of charcoal is insufficient to support the burden inside the furnace, allowing it to replace only around 10% of the coke introduced at the top. Therefore, the industry has adopted the injection of pulverized charcoal at the tuyeres, replacing the pulverized coal injection. Typical injection rates for charcoal range from 100 to 150 kg/t_{HM}. Some authors have proposed co-injecting charcoal with the syngas produced during the pyrolysis process to enhance biomass utilization (Fig. 2) [29].

From this comprehensive literature review, it is evident that existing solutions for conventional blast furnaces offer CO_2 reductions in the range of 30% – 45%, falling short of the ambitious European targets for net zero emissions by 2050. Motivated by this gap, our study aims to push the boundaries by integrating state-of-the-art solutions with biomass pyrolysis to achieve further reductions in CO_2 emissions. In this research, we introduce and evaluate, for the first time, the integration of all the previously mentioned alternatives for CO_2 reduction in blast furnaces: top gas recycling, oxygen blast furnace, power to gas, and charcoal. This innovative system seeks to achieve the maximum possible CO_2 reduction without relying on geological storage. We have chosen pinus radiata waste as the biomass source, which is abundantly available in Chile and Spain but is not currently valorized. The central hypothesis we aim to test is whether the proposed system can significantly surpass current solutions in reducing CO_2 emissions.

2.1. Integration of power to gas, biomass pyrolysis and oxygen blast furnace

The innovative concept presented in this paper integrates top gas recycling, oxygen blast furnaces, power to gas technology, and biomass utilization (via charcoal and syngas from a pyrolysis process). Due to the intricacies of this combination, there are various integration options that warrant consideration.

For instance, with regard to top gas recycling, the recirculated gas can be injected at various points: the tuyeres (lower part), shaft (middle part), preparation zone (upper part), or a combination thereof. Injecting the recirculated gas at the tuyeres facilitates effective interaction between the reducing gas and the solids but comes at the cost of decreasing the flame temperature, which must not fall below 2000 °C for technical reasons. Conversely, injections at mid-shaft avoid reducing the flame temperature, but the injection becomes peripheral, limiting the penetration and diffusion of the gas to the center of the descending burden, resulting in poor solid–gas interaction [6]. In the case of upper injections, the role of the recirculated gas is primarily to preheat the

descending solids, addressing the lack of sensible heat no longer provided by N_2. As the gas is not intended to serve as a reducing agent, the diffusion of the gas towards the center is not critical, and the presence of CO_2 is not problematic [6]. However, the drawback of upper recycling is the potentially excessively high temperature at the tuyeres if no other gases are concurrently injected.

Regarding methanation, various gases can serve as the carbon source for synthetic natural gas production. Options include pure CO_2 from the carbon capture stage (as illustrated in Fig. 2), the treated blast furnace gas (sweet gas) from this stage, or the blast furnace gas itself (particularly when it lacks N_2 content under oxy-fuel regime). Utilizing pure CO_2 simplifies the process as no other chemical species would influence methanation. In the case of sweet gas methanation, this approach reserves pure CO_2 for geological storage while maintaining carbon from CO in a closed loop. If blast furnace gas is used in methanation, the need for a carbon capture stage is eliminated, and all the heat generated during methanation becomes available for integration into other processes.

In the existing literature, the integration of oxygen blast furnaces and power to gas has received limited attention, with only a handful of authors exploring this combination. Some studies have employed top gas recycling at the tuyeres [21,24,25], others at the preparation zone [30,31], and only one has investigated the dual recycling approach at both the tuyeres and preparation zone [32]. Additionally, these authors have considered methanation using various carbon sources, including pure CO_2 from the carbon capture stage [21,25,30,32], sweet gas from carbon capture [25], or the blast furnace gas itself [24,25,31]. In most cases, synthetic natural gas was injected at the tuyeres, likely due to the limited solid–gas interaction observed when the reducing gas is introduced at the shaft. When comparing the outcomes from these studies across potential integration options, the combination of upper recycling with direct methanation of blast furnace gas under oxy-fuel regime stands out for achieving the most significant reduction in CO_2 emissions. In this configuration, the CO_2 emissions of the blast furnace were reported as 747 kg_{CO2}/t_{HM} [31], representing a remarkable 44% reduction compared to conventional air-blown blast furnaces [33]. Importantly, this reduction in emissions does not necessitate geological storage.

The proposed novel concept adopts the best configuration identified in the literature to enhance CO_2 reduction beyond the 44% achieved, primarily through the incorporation of charcoal and syngas. Additionally, the choice of combining upper recycling with direct methanation eliminates the need for a carbon capture stage, enhancing the overall simplicity of the system. The process flow diagram of the novel concept is illustrated in Fig. 3. It is worth noting that the syngas derived from the pyrolysis process may contain substantial H_2 content, contributing to a reduction in the power capacity and electricity consumption of the electrolyzer—a significant advantage given that electricity consumption is a major drawback in such systems.

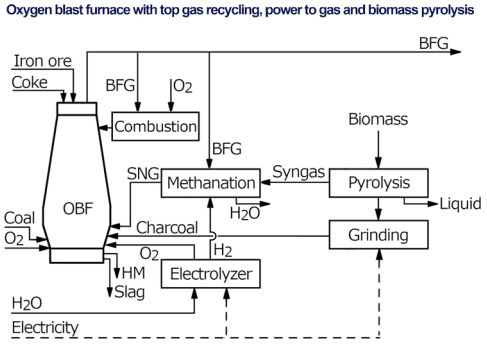

Fig. 3. Process flow diagram of a novel concept for the reduction of CO_2 emissions in blast furnace ironmaking, combining top gas recycling, oxy-fuel regime, power to gas, and biomass pyrolysis.

3. Methods

3.1. Case studies

The process flow diagram depicted in Fig. 3 will undergo evaluation for the pyrolysis of pinus radiata under various operating conditions. The pyrolysis temperature plays a crucial role in determining the proportions and compositions of solid, liquid, and gas products. These parameters, in turn, impact the required production of H_2 in the electrolyzer, the flow of blast furnace gas applicable in methanation, and the quantity of fossil fuel that can be substituted. Consequently, these factors will influence the amount of biomass that can be utilized, ultimately shaping the final CO_2 emissions.

Pinus radiata was chosen due to its extensive availability in Chile, with an estimated resource quantity of 1.3 – 2.3 million tons per year [34–36]. The data for pinus radiata were sourced from the experiments conducted by Solar et al. (Table 1) [37]. These experiments utilized waste chips derived from forest thinning, specifically the rejected fraction that was too small for boilers (i.e., <6 cm) [38]. Solar et al.'s experimental setup comprised two connected reactors: a pyrolysis reactor and a vapors treatment reactor operating at 800 °C. The pyrolysis reactor, an externally heated tubular screw reactor (auger reactor), allowed independent control of temperature and rotation speed of the

Table 1
Characterization of the biomass resource and the pyrolysis products for the different case studies.

	Case 1	Case 2	Case 3	Case 4
Biomass	Pinus radiata	Pinus radiata	Pinus radiata	Pinus radiata
Proximate analysis (wt%)				
Moisture	10.6	10.6	10.6	10.6
Volatile matter	70.7	70.7	70.7	70.7
Ash	0.6	0.6	0.6	0.6
Fixed carbon	18.1	18.1	18.1	18.1
Elemental analysis (wt% daf)				
C	47.8	47.8	47.8	47.8
H	7.6	7.6	7.6	7.6
O	44.6	44.6	44.6	44.6
N	0.0	0.0	0.0	0.0
HHV (MJ/kg)	16.4	16.4	16.4	16.4
Pyrolysis process				
Type	Slow	Slow	Slow	Slow
Temperature (°C)	300	500	700	900
Time (min)	30	30	30	30
Yield (wt.%)				
Solid	53.8	31.4	24.3	19.3
Gas	9.6	31.8	50.8	70.0
Liquid	36.6	36.8	24.9	10.7
Solid phase				
Proximate analysis (wt%)				
Moisture	4.8	4.8	2.1	1.3
Volatile matter	47.6	20.3	10.6	7.3
Ash	1.8	3.3	4.2	5.1
Fixed carbon	45.8	71.6	83.1	86.3
Elemental analysis (wt% daf)				
C	76.0	94.5	99.0	99.4
H	10.1	2.3	0.4	0.1
O	13.7	3.2	0.5	0.5
N	0.2	0.0	0.1	0.0
HHV (MJ/kg)	27.4	31.5	32.8	32.0
Gas phase				
Compound (vol%)				
H_2	8.0	21.9	39.0	42.7
CO	47.0	22.2	29.2	32.6
CO_2	28.1	43.4	16.3	14.2
CH_4	9.1	10.9	14.5	9.9
C_2H_4	7.1	1.1	0.7	0.5
C_2H_6	0.8	0.5	0.3	0.1
HHV (MJ/kg)	11.9	8.7	18.0	17.3
HHV (MJ/Nm^3)	14.3	10.0	13.8	12.7
Reference	[37]	[37]	[37]	[37]

screws. The external electrical heating was divided into four individual zones with separately adjustable temperatures. The biomass-feeding rate was set at 0.65 g/min. Once the biomass reached the end of the reactor, the resulting solid (charcoal) was collected into a closed heated hopper, while the vapors were directed to the tubular vapors reactor. In this subsequent stage, the produced vapors were separated into bio-oils and pyrolysis gases. The vapor treatment process improved gas yields and quality, thereby reducing the formation of liquids [37]. Given that the primary resources in the blast furnace integration are solid and gas products, this additional treatment holds particular significance for our study. Bio-oils were collected in a glass fiber extraction thimble located in the condensation system (metal vessel at 1 °C). The gases underwent cleaning (activated carbon and silica gel columns, isopropyl alcohol bubbler, and particle filter) and were collected in gas bags. Steady-state experiments had a duration of 150 min. The complete ash composition of the produced charcoal can be found in [39]. For further details on the plant setup used by Solar et al., refer to [40].

For the comparison with a conventional air-blown blast furnace, the chosen coal was sourced from [41,42], and its composition is provided in Table 2.

Table 2
Characterization of the pulverized coal used in Aspen Plus for the air-blown blast furnace [41,42].

	Pulverized coal
Proximate analysis (wt%)	
Moisture	1.2
Volatile matter	17.2
Ash	10.8
Fixed carbon	70.8
Elemental analysis (wt% daf)	
C	87.2
H	4.7
O	5.8
N	1.8
S	0.5
HHV (MJ/kg) (Aspen Plus)	33.6

3.2. Aspen plus model

The utilization of various charcoals and syngas directly impacts both the methanation stage and the blast furnace. Each case study will yield different amounts and compositions of blast furnace gas, thereby influencing the requirements in the methanation stage. However, the pyrolysis process remains unaffected by variations in the blast furnace. As a result, the Aspen Plus model segregates the blocks of pyrolysis and grinding, treating charcoal and syngas as inputs to the model (refer to data from Table 1).

The blast furnace model is built upon the extended operating line methodology, a recent development by Bailera et al. [43]. This methodology serves as a generalization of the operating line initially proposed by Rist in 1967 [21,44]. It enables the prediction of blast furnace behavior when operating conditions are altered, even in scenarios involving oxy-fuel regimes and multiple gas and solids injections at different zones. The implementation of the extended operating line methodology is carried out in Aspen Plus, with individual models for the upper, mid, and lower zones of the blast furnace, the latter encompassing the raceways (see Fig. 4). The model involves 10 inlet mass

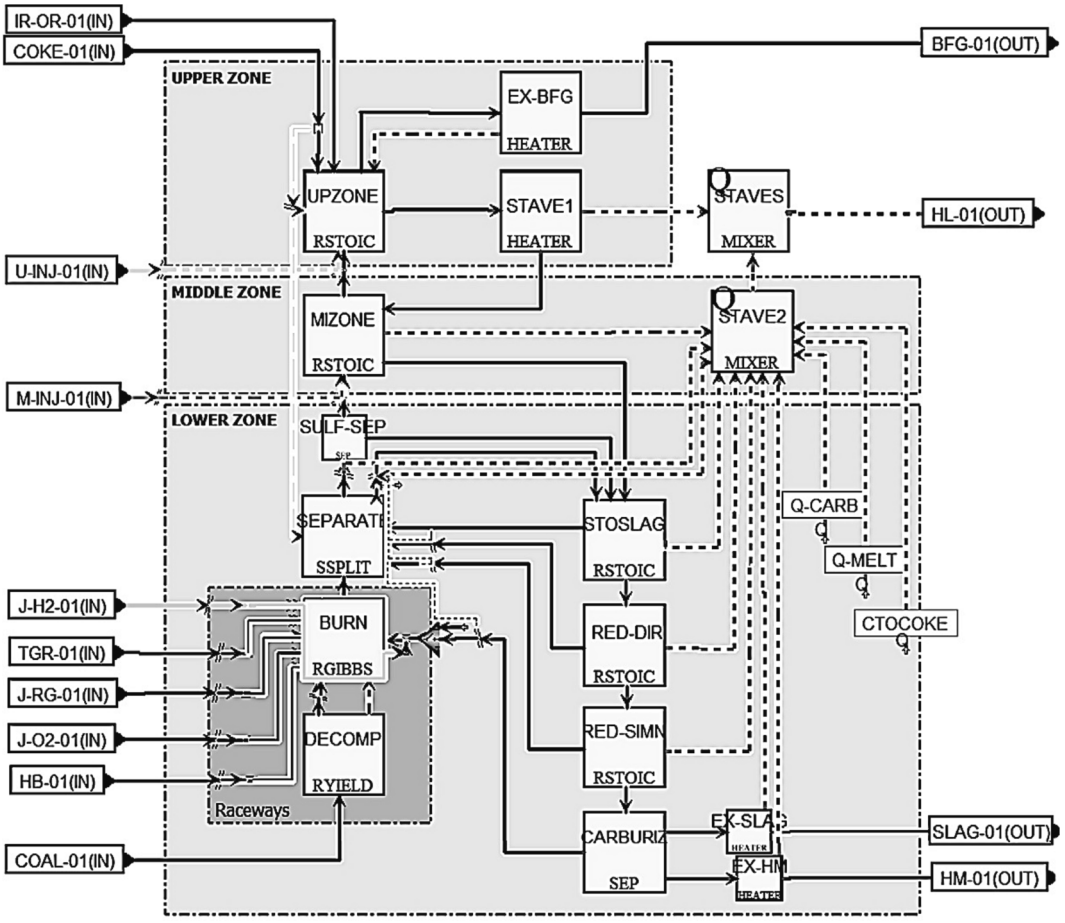

Fig. 4. Process flow diagram of the blast furnace in Aspen Plus.

Table 3
Summary of model input / output data regarding the streams crossing the boundary of the blast furnace.

Stream	Description	Flow	Composition	Temperature
IR-OR-01	Iron ore	Input	Input	Input
COKE-01	Coke	Output	Input	Input
HB-01	Air + moisture	Output	Input	Input
COAL-01	Pulverized charcoal injection at tuyeres	Input	Input	Input
J-O2-01	O_2 injection for enrichment at tuyeres	Input	Input	Input
J-H2-01	H_2 injection at tuyeres	Input	Input	Input
J-RG-01	Gas injection at tuyeres	Input	Input	Input
TGR-01	Top gas recirculation injected at tuyeres	Input	Input	Input
M−INJ−01	Gas injection at mid shaft	Input	Input	Input
U-INJ-01	Gas injection at upper part	Input	Input	Input
HM-01	Hot metal	Output	Input	Input
SLAG-01	Slag	Output	Output	Input
BFG-01	Blast furnace gas	Output	Output	Output
HL-01	Heat removed by the staves	Input	–	–

streams, three outlet mass streams, and one outlet heat stream that traverse the blast furnace boundary. It calculates the mass flow of coke, air, hot metal, slag, and blast furnace gas as a function of the temperature of the thermal reserve zone, chemical efficiency, heat removed by the staves (in both the preparation and elaboration zones), and the inputs specified in Table 3. Detailed descriptions of the model can be found in the author's previous papers [33,43], and all simulation files are available as supplementary material.

The methanation plant is based on technology developed by Hitachi Zosen Corporation (Fig. 5). Their technology involves two shell-and-tube type exchange reactors operating at 5 bar and 250 °C, with an intermediate condensation stage. The resulting synthetic natural gas has a final CH_4 content of 98.5 vol% and an H_2 content of 1.3 vol%, both in dry basis [45]. The corresponding Aspen Plus model includes two 2-stage compressors for the inlet CO_2 and H_2, with compression ratios of 2.5:1 and 2:1, along with intermediate cooling at 60 °C. It also features two RGibbs equilibrium reactors for the methanation stages (at 250 °C and 5 bar), two Flash reactors for water condensation after each methanator (at 50 °C and 35 °C), and two preheating exchangers before each methanator (at 250 °C).

3.3. Key performance indicators

To characterize and compare the four case studies, we have defined 12 key performance indicators (Table 4). These indicators encompass various aspects, including the flame temperature inside the blast furnace, fuel consumption, the sizing of the power to gas plant, required top gas recycling, and environmental and energy performance. These parameters are parametrized based on the biomass consumed in the pyrolysis process (providing an indication of the level of integration) and the blast furnace gas sent to methanation (highlighting the significance of the carbon loop).

KPI01 to KPI07 are derived directly from the Aspen Plus simulation based on the extended operating line model. KPI01 represents the flame temperature, a critical factor that determines the maximum integration potential. The temperature decreases when methane and charcoal are injected into the blast furnace, but it should never fall below 2000 °C for technical reasons [46]. Consequently, there is a maximum limit on the amount of biomass that can be used in blast furnaces. KPI02, KPI03, and KPI04 indicate the fuel consumptions of the blast furnace, representing synthetic natural gas, charcoal, and coke, respectively. A lower KPI04 implies reduced fossil fuel usage in the blast furnace. KPI05 and KPI06 are related to the power to gas plant, indicating the installed power capacity and the amount of O_2 that can be saved in the air separation

Table 4
Parametric variables and key performance indicators for assessing the novel integration of Fig. 3.

Type	Description	Units
Parametric	Biomass consumed in pyrolysis	kg/t_{HM}
Parametric	BFG recirculated through methanation	kg/t_{HM}
KPI01	Flame temperature	°C
KPI02	Synthetic natural gas injected at tuyeres	kg/t_{HM}
KPI03	Charcoal injected at tuyeres	kg/t_{HM}
KPI04	Coke consumption	kg/t_{HM}
KPI05	Electrolysis power	MW/(t_{HM}/h)
KPI06	O_2 from the air separation unit	kg/t_{HM}
KPI07	Energy available in BFG for downstream processes	MJ/t_{HM}
KPI08	Gross CO_2 emissions	kg/t_{HM}
KPI09	Net CO_2 emissions (deducting CO_2 from biomass)	kg/t_{HM}
KPI10	Electricity consumed	MJ/t_{HM}
KPI11	Thermal energy consumed	MJ/t_{HM}
KPI12	Specific primary energy consumption per unit of CO_2 avoided (SPECCA)	MJ/kg_{CO2}

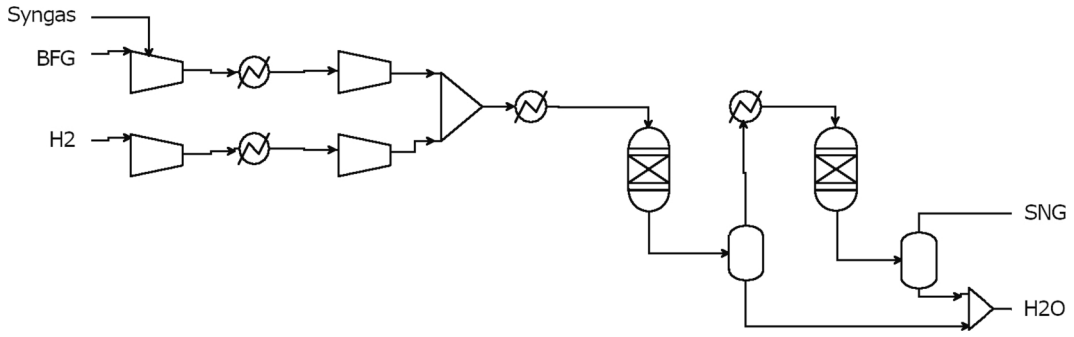

Fig. 5. Process flow diagram of the methanation plant in Aspen Plus.

unit through electrolysis. We assumed an electrolysis consumption of 4.5 kWh/Nm^3, corresponding to a commercial containerized PEM in the MW scale [47]. Finally, KPI07 quantifies the energy contained in the blast furnace gas exiting the system, which can be utilized for downstream processes in the steel plant.

KPI08 to KPI12 are calculated using the results from the Aspen Plus simulation. KPI08 and KPI09 pertain to the environmental performance of the novel integration, providing gross and net CO_2 equivalent emissions. These values are computed under the assumption that the CO content of the blast furnace gas will ultimately be converted to CO_2 after combustion. The stream used to quantify emissions is the BFG not utilized in either top gas recycling or methanation (see Fig. 3). The only distinction between gross (Eq.(1)) and net CO_2 emissions (Eq.(2)) is that the latter deducts the carbon originating from biomass since it is considered CO_2-neutral (i.e., the carbon from the syngas and the charcoal).

$$\mathrm{KPI08} = \sum_{i=CO_2,CO} n_{BFG,i} M_{CO2} \quad (1)$$

$$\mathrm{KPI09} = \mathrm{KPI08} - \left(\sum_{i=CO_2,CO,CH_4} n_{SYN,i} + \sum_{i=C_2H_4,C_2H_6} 2n_{SYN,i} + n_{CC,C} \right) M_{CO2} \quad (2)$$

KPI10 and KPI11 are associated with the electricity and thermal energy consumption of the system. The electricity consumption is the sum of the electrolyzer and air separation unit consumptions (Eq.(3)), with the expectation that electrolysis will significantly contribute to the overall consumption. We assume a specific consumption of 380 kWh/t_{O2} for the air separation unit [48].

$$\mathrm{KPI10} = \left(\mathrm{KPI05} + \frac{380}{10^6} \mathrm{KPI06} \right) 3600 \quad (3)$$

Regarding thermal consumption, it is solely attributed to the pyrolysis process. Typical estimates from the literature range from 6% to 15% of the higher heating value (HHV) of biomass [49]. In this study, we adopt the less optimistic value of 15%, ensuring that the energy penalties we derive correspond to the worst potential scenario (Eq.(4)).

$$\mathrm{KPI11} = \frac{\mathrm{KPI03}}{Y_S} \mathrm{HHV_B} 0.15 \quad (4)$$

Lastly, KPI12 is the SPECCA, which stands for Specific Primary Energy Consumption per unit of CO_2 Avoided. For the calculation of SPECCA, we use the net CO_2 emissions (Eq.(5)).

$$\mathrm{KPI12} = \frac{\mathrm{KPI10} + \mathrm{KPI11}}{1336 - \mathrm{KPI09}} \quad (5)$$

The value of 1336 kg_{CO2}/t_{HM} corresponds to a conventional air-blown blast furnace with pulverized coal injection. This value was obtained in previous articles by the authors [33]. The same base case simulation is used in the present paper for comparison purposes.

4. Results and discussion

All results are presented as a function of biomass consumption and the blast furnace gas directed to methanation. The integration analysed is the one depicted in Fig. 3, assuming no pulverized coal is injected. Subsequently, these results are compared with those of the conventional air-blown blast furnace and with other oxygen blast furnaces from the literature.

4.1. Maximum potential of integration, limited by the flame temperature (KPI01)

The initial stage of the parametric analysis assumes no biomass consumption and no blast furnace gas sent to methanation. Since pulverized coal is also excluded, the flame temperature starts at an exceptionally high level (3,125 °C). This aligns with an oxy-fuel regime where no input material serves as a heat sink at the tuyeres. As biomass is introduced, the flame temperature gradually decreases. The steepest decline is observed for charcoals derived from pyrolysis at 300 °C, resulting in a reduction rate of approximately 4.2 °C per kilogram of biomass consumed in pyrolysis (Fig. 6). This is primarily due to the elevated H:C and O:C ratios of this charcoal. The subsequent charcoal, obtained from pyrolysis at 500 °C, lowers the flame temperature by 2.1 °C per kilogram of biomass consumed. This charcoal exhibits H:C and O:C ratios more akin to those of fossil coal (Table 2). With pyrolysis at 700 °C, the H:C and O:C ratios of the charcoal continue to decrease, allowing for more substantial charcoal injections (flame temperature decreases by 1.9 °C per kilogram of biomass used in pyrolysis). Further elevating the operating temperature of pyrolysis (900 °C) does not significantly alter the composition of the charcoal but yields notably higher gas product outputs. Consequently, more renewable fuel is injected into the blast furnace per kilogram of biomass, leading to a faster decrease in the flame temperature. With 2000 °C as the lower limit for the flame temperature, the maximum biomass consumption is 194 kg/t_{HM}, 370 kg/t_{HM}, 532 kg/t_{HM}, and 408 kg/t_{HM} for Cases 1 to 4, respectively (Table 1). Assuming a typical blast furnace production of 500 t_{HM}/h [25], the required biomass supply falls within the range of 97 to 266 t/h, corresponding to an annual consumption of 0.81 – 2.23 Mt/y. The annual availability of Pinus radiata in Chile ranges from 1.3 to 2.3 Mt/y, potentially providing renewable fuel for 1 – 3 blast furnaces each year.

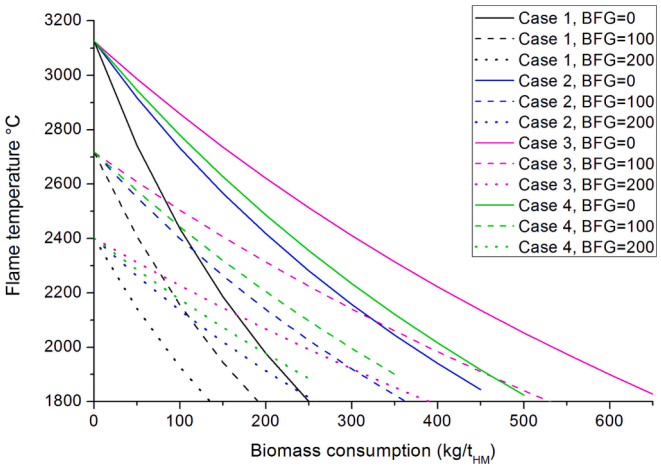

Fig. 6. Flame temperature (KPI01) vs. biomass consumption in pyrolysis (Table 1) and BFG consumed in methanation, for the novel integration of oxygen blast furnaces with pyrolysis and power to gas (Fig. 3).

In situations where biomass availability is limited, the novel concept facilitates carbon recycling through methanation. It introduces synthetic natural gas, produced by utilizing blast furnace gas and hydrogen derived from renewable electricity. The injection of synthetic natural gas results in a reduction of flame temperature by 2.3 – 3.3 °C per kilogram of blast furnace gas sent to methanation. For instance, when consuming 200 kg of BFG, biomass requirements are only 0.34 – 1.03 Mt/y, at the limit of a 2000 °C flame temperature.

4.2. Fuel consumptions in the blast furnace (KPI02, KPI03 and KPI04)

In the simulations, we assume that all the charcoal and syngas obtained from pyrolysis are utilized in the integration. However, as the syngas is mixed with blast furnace gas for methanation, the final solid/gas ratio injected into the blast furnace may not necessarily match the pyrolysis solid/gas yield ratio. Concerning the synthetic natural gas injected at the tuyeres, its increase with biomass consumption is more rapid for pyrolysis at higher temperatures due to the higher syngas yield

ratio (Fig. 7). However, the SNG injected increases uniformly for all cases with the BFG sent to methanation (around 40 kg_{SNG}/kg_{BFG}). In the case of charcoal, its amount increases with biomass but decreases at higher pyrolysis temperatures because the solid yield ratio is lower. In terms of the quantity of charcoal injected, the BFG sent to methanation has no influence (Fig. 8). For the technical limit of 2000 °C, the charcoal injection ranges between 36 and 129 kg/t_{HM}, and the SNG injection between 10 and 148 kg/t_{HM}, depending on the case study. Considering both reducing agents together, the mass flow of injected renewable fuel ranges between 114 and 273 kg/t_{HM}. The lower value corresponds to Case 0 (pyrolysis at 300 °C) with no BFG sent to methanation, and the higher value corresponds to Case 3 (pyrolysis at 700 °C) with no BFG sent to methanation.

Regarding fossil fuel, coke consumption varies based on the amount and type of reducing agent injected at the tuyeres (Fig. 9). To analyze this behavior, it is useful to compute the fossil fuel replacement ratio, which is the quotient between the avoided coke and the material used to replace it. Focusing on the reducing agents from the pyrolysis process, the replacement ratios are −0.38 $kg_{COKE}/kg_{BIOMASS}$, 0.10 $kg_{COKE}/kg_{BIOMASS}$, 0.61 $kg_{COKE}/kg_{BIOMASS}$, and 0.65 $kg_{COKE}/kg_{BIOMASS}$ for Case 1, 2, 3, and 4, respectively. Differences arise from the gas/solid yield ratio and the charcoal composition. Higher gas yield ratio and higher carbon content in charcoal result in better replacement ratios. Considering the reducing agent from the recycling of BFG, the ratios are 0.44 kg_{COKE}/kg_{BFG}, 0.43 kg_{COKE}/kg_{BFG}, 0.41 kg_{COKE}/kg_{BFG}, and 0.41 kg_{COKE}/kg_{BFG} for Case 1, 2, 3, and 4. These values are very similar because all correspond to SNG injections with CH_4 contents above 95 vol%. The only situation where coke consumption might increase is for Case 1 with high biomass consumption and/or low BFG recycling. This is related to the excessively drop in flame temperature shown in Fig. 6, originated by the lack of heat in the lower zone, which must be palliated by introducing more coke at the top. In all other situations, coke is expected to decrease, to a greater or lesser extent according to the mentioned replacement ratios. It can be observed that for Case 2 (pyrolysis at 500 °C), it is better to prioritize BFG recycling, contrary to Case 3 and Case 4 (pyrolysis at 700 °C and 900 °C) where biomass consumption leads to greater coke savings.

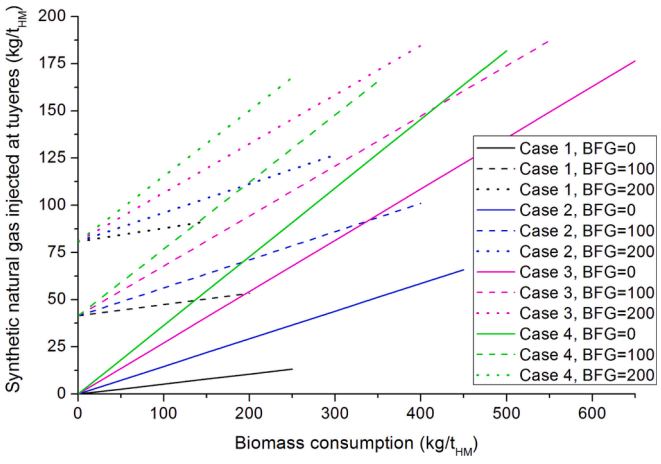

Fig. 7. Synthetic natural gas injected at tuyeres (KPI02) vs. biomass consumption in pyrolysis (Table 1) and BFG consumed in methanation, for the novel integration of oxygen blast furnaces with pyrolysis and power to gas (Fig. 3).

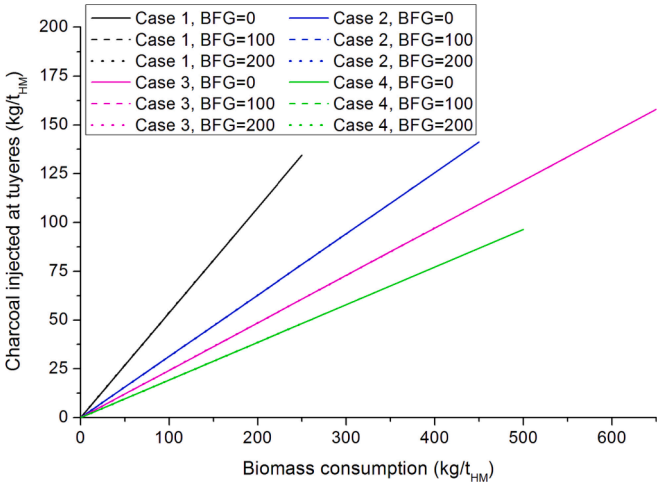

Fig. 8. Charcoal injected at tuyeres (KPI03) vs. biomass consumption in pyrolysis (Table 1) and BFG consumed in methanation, for the novel integration of oxygen blast furnaces with pyrolysis and power to gas (Fig. 3).

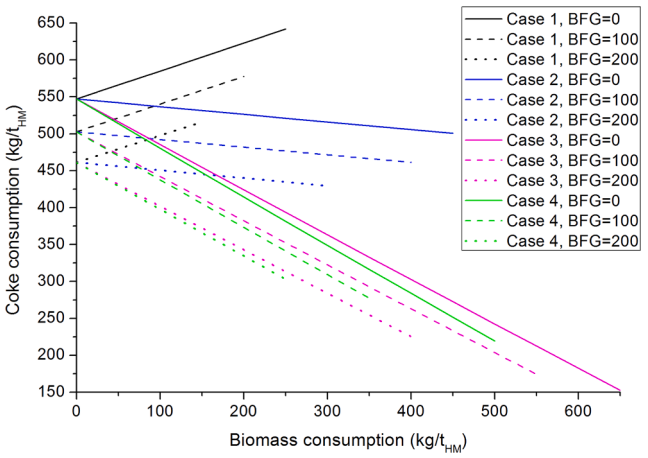

Fig. 9. Coke consumption (KPI04) vs. biomass consumption in pyrolysis (Table 1) and BFG consumed in methanation, for the novel integration of oxygen blast furnaces with pyrolysis and power to gas (Fig. 3).

Considering the technical limitation of a 2000 °C flame temperature, the minimum coke consumption is 223 kg/t_{HM}, observed in Case 3 without sending BFG to methanation (i.e., the scenario with the highest injection of reducing agents at the tuyeres, consisting of 274 kg/t_{HM} of charcoal plus SNG). This signifies a 23% reduction in coke consumption compared to air-blown blast furnaces and a 54% decrease in fossil fuel consumption (conventional air-blown BF consumes 288 kg/t_{HM} of coke and 200 kg/t_{HM} of pulverized coal).

4.3. Power to gas plant (KPI05 and KPI06)

Characterizing the power to gas plant is crucial in these integrations, given that a significant portion of the capital expenditure is associated with the electrolyzer, and the primary operating expenditure is linked to electricity consumption [30]. The electrolyzer size required for methanation increases with higher syngas production in pyrolysis, which is influenced by factors such as biomass consumption and gas yield rates during pyrolysis, varying notably between different case studies (Fig. 10). The electrolysis capacity grows in the range of 0.8 to 3.6 $kW/(t_{HM}/h)$ per kg of biomass consumed, depending on the case. Similarly, when BFG is sent to methanation, the required H_2 for the process increases. However, as the BFG composition remains consistent across most cases, the increment in electrolysis size per kg of BFG sent to methanation is approximately 9 $kW/(t_{HM}/h)$ in all case studies. Assuming a typical blast furnace with a production rate of 500 t_{HM}/h and considering the 2000 °C flame temperature limitation, the required electrolysis capacity ranges from 100 MW to 1200 MW, depending on the case. Case 1 (300 °C pyrolysis) without BFG sent to methanation demands the least electrolysis capacity, while Case 4 (900 °C pyrolysis)

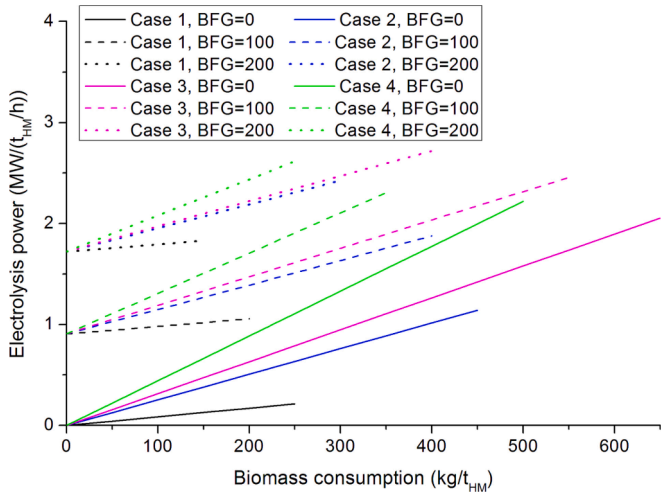

Fig. 10. Electrolysis power (KPI05) vs. biomass consumption in pyrolysis (Table 1) and BFG consumed in methanation, for the novel integration of oxygen blast furnaces with pyrolysis and power to gas (Fig. 3).

with 200 kg of BFG sent to methanation requires the highest capacity. These electrolyzer capacities align with some of the largest planned green hydrogen projects worldwide.

One advantage of integrating electrolysis is the availability of O_2, which helps to reduce the electricity consumption of the air separation unit providing the oxy-fuel regime. However, in Case 1 and Case 2, despite O_2 being available from the electrolyzer, ASU production had to be increased under certain operating conditions (Fig. 11). Similar to KPI04 (coke consumption), we examine the fossil fuel replacement ratios to understand this behavior. In this case, replacement ratios are computed based on the actual mass flow of reducing agents entering the blast furnace. Considering charcoal and SNG from pyrolysis, the replacement ratios are -0.64 kg_{COKE}/kg_{CC+SNG}, 0.22 kg_{COKE}/kg_{CC+SNG}, 1.18 kg_{COKE}/kg_{CC+SNG}, and 1.17 kg_{COKE}/kg_{CC+SNG} for Case 1, 2, 3, and 4, respectively. Cases with replacement ratios below 1 (increasing total BF fuel consumption) require an increased O_2 production in the ASU at a faster rate than saved by the electrolyzer. Looking at SNG from recycled blast furnace gas, the replacement ratio is 1.03 kg_{COKE}/kg_{SNG} for all cases. Thus, increasing BFG recycling helps saving O_2 in the ASU, as illustrated in Fig. 11. At the technical point of a 2000 °C flame temperature, the configuration with the lowest ASU consumption is Case 4 with 200 kg/t_{HM} of BFG sent to methanation. This requires only 107 kg/t_{HM} of O_2 produced by the ASU, equivalent to 146 MJ/t_{HM} of electricity.

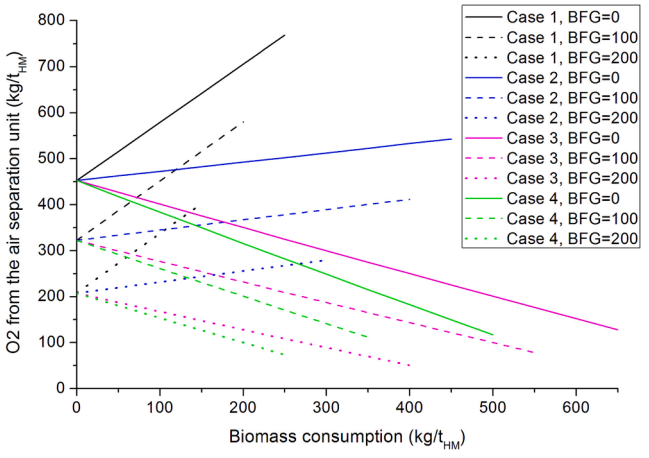

Fig. 11. O_2 from the air separation unit (KPI06) vs. biomass consumption in pyrolysis (Table 1) and BFG consumed in methanation, for the novel integration of oxygen blast furnaces with pyrolysis and power to gas (Fig. 3).

4.4. Energy available in BFG for downstream processes (KPI07)

Blast furnace gas, also known as top gas, is a valuable fuel extensively utilized downstream in integrated steel plants, providing approximately 5,000 MJ/t_{HM} of thermal energy to various processes and ensuring industry self-sufficiency. However, the novel proposal, like any oxygen blast furnace, reduces the availability of BFG as TGR concepts consume part of the BFG to maintain proper temperatures within the furnace. The proportion of blast furnace gas recirculated in the upper zone is depicted in Fig. 12 as a percentage of the total BFG produced in the blast furnace. This percentage decreases with biomass consumption and BFG recycling. The injection of reducing agents in the tuyeres enhances the flow of ascending gas inside the blast furnace, reducing the lack of sensible heat in the upper zone and consequently decreasing the necessity for top gas recycling.

Considering the limitation of a 2000 °C flame temperature, the available energy proves sufficient for the self-sufficiency of downstream processes in all cases (ranging from 5,752 to 7,771 MJ/t_{HM}) (Fig. 13), despite the utilization of BFG in the integration. Furthermore, the surplus thermal energy available in the form of BFG could potentially cover

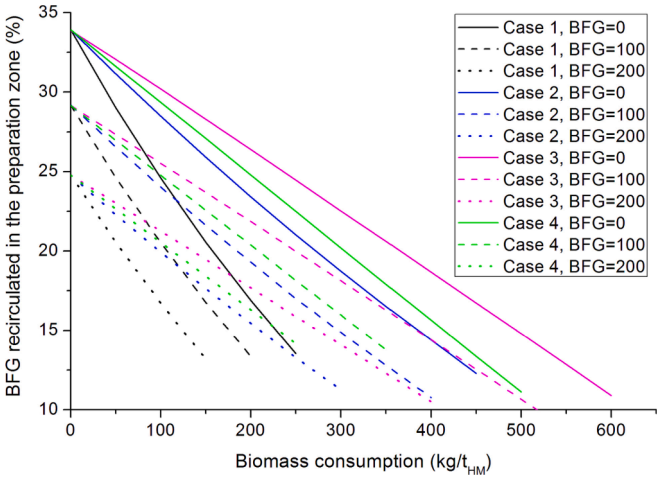

Fig. 12. BFG recirculated in the preparation zone (%) vs. biomass consumption in pyrolysis (Table 1) and BFG consumed in methanation, for the novel integration of oxygen blast furnaces with pyrolysis and power to gas (Fig. 3).

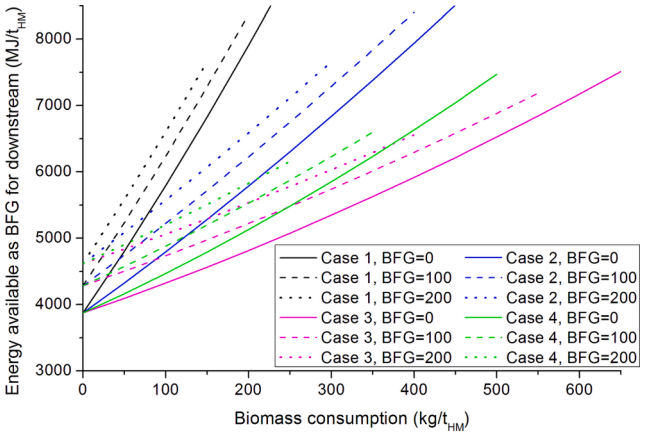

Fig. 13. Energy available in the form of BFG for downstream processes (KPI07) vs. biomass consumption in pyrolysis (Table 1) and BFG consumed in methanation, for the novel integration of oxygen blast furnaces with pyrolysis and power to gas (Fig. 3).

the thermal requirements of pyrolysis. However, this self-sufficiency does not extend to covering the electricity consumption for the electrolyzer. The case that provides the least energy in the form of BFG is Case 4 with 200 kg of BFG sent to methanation, while the case with the highest energy as BFG is Case 1 with no BFG sent to methanation.

4.5. Environmental performance (KPI08 and KPI09)

The primary objective of researching new blast furnace concepts is to reduce CO_2 emissions. Initially, we examine gross emissions, encompassing all the CO_2 released due to the BFG exiting the system as depicted in Fig. 3. This includes both CO_2 and CO, the latter of which transforms into CO_2 when using BFG as fuel (Eq.(1)). Gross CO_2 emissions are closely linked to the coke replacement ratios discussed in section 4.3, and thus, the O_2 required from the ASU (notably seen in the similar trends of KPI08 in Fig. 14and KPI06 in Fig. 11). Configurations with replacement ratios below 1 result in higher fuel consumption in the blast furnace, leading to increased CO_2 emissions. This is evident in Case 1 and Case 2, where pyrolysis plays a significant role in the integration (i.e., high biomass consumption and low BFG recycling). However, since biomass (a CO_2-neutral fuel) is utilized to replace coke, we can calculate net CO_2 emissions (Eq.(2)), deducting the carbon from biomass from gross emissions. This allows us to observe that Case 3 and Case 4 quickly reduce their emissions below the typical emissions of conventional air-blown blast furnaces (i.e., below 1336 kg/t_{HM}) (Fig. 15). In contrast, Case 1 and Case 2 cannot compete with well-established air-blown BF, either because net CO_2 emissions increase compared with conventional BF or because the CO_2 reduction is limited (4.3%) and not justifiable. Considering the flame temperature limitation (2000 °C), the maximum CO_2 abatement in Case 3 is 58%, and in Case 4 is 45%, both scenarios occurring when no BFG is sent to methanation.

4.6. Energy performance (KPI10, KPI11 and KPI12)

When targeting CO_2 reduction, a crucial factor is the energy penalization. In the proposed integration, there is additional electricity consumption for the production of green H_2 used in methanation and for O_2 production for the oxy-fuel regime (Fig. 16). Additionally, there is extra thermal energy consumption for the pyrolysis process (Fig. 17). Electricity consumption increases more rapidly with the rise in BFG recycling (25 – 31 MJ/t_{HM} per kg of BFG sent to methanation) compared to the increase in biomass consumption (4 – 15 MJ/t_{HM} per kg of biomass used in pyrolysis), mainly due to the higher demand for H_2 in the former case. In terms of thermal energy consumption, the assumption was to consider 15% of the higher heating value of the biomass as the energy required for pyrolysis. Due to this assumption, all cases exhibit the same energy consumption, growing at a rate of 2.5 MJ/t_{HM} per kg of biomass consumed in pyrolysis. Therefore, in terms of efficiency, it is preferable to prioritize biomass consumption over carbon recycling.

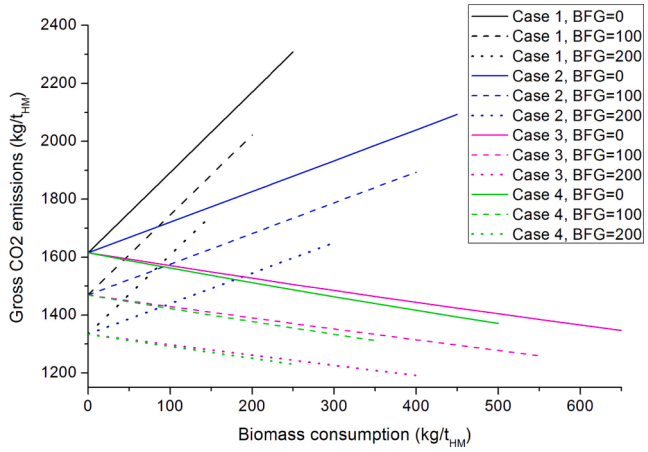

Fig. 14. Gross CO_2 emissions (KPI08) vs. biomass consumption in pyrolysis (Table 1) and BFG consumed in methanation, for the novel integration of oxygen blast furnaces with pyrolysis and power to gas (Fig. 3).

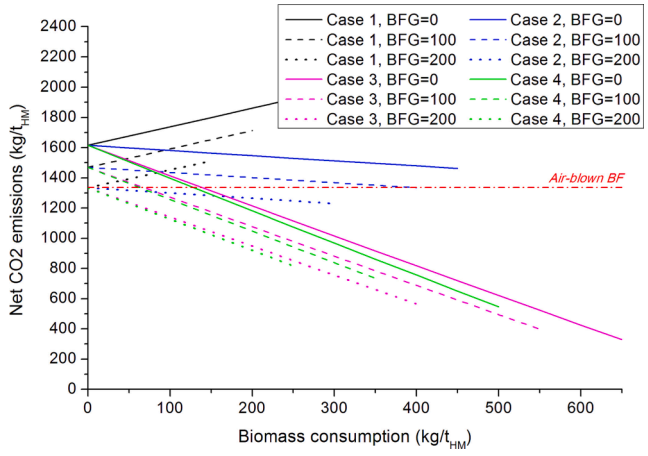

Fig. 15. Net CO_2 emissions (KPI09) vs. biomass consumption in pyrolysis (Table 1) and BFG consumed in methanation, for the novel integration of oxygen blast furnaces with pyrolysis and power to gas (Fig. 3).

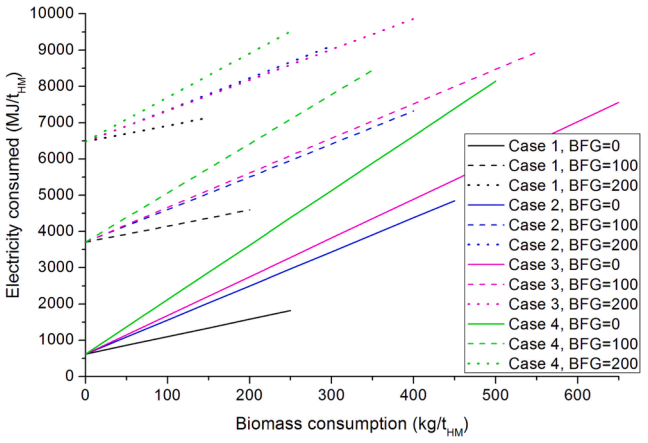

Fig. 16. Electricity consumed (KPI10) vs. biomass consumption in pyrolysis (Table 1) and BFG consumed in methanation, for the novel integration of oxygen blast furnaces with pyrolysis and power to gas (Fig. 3).

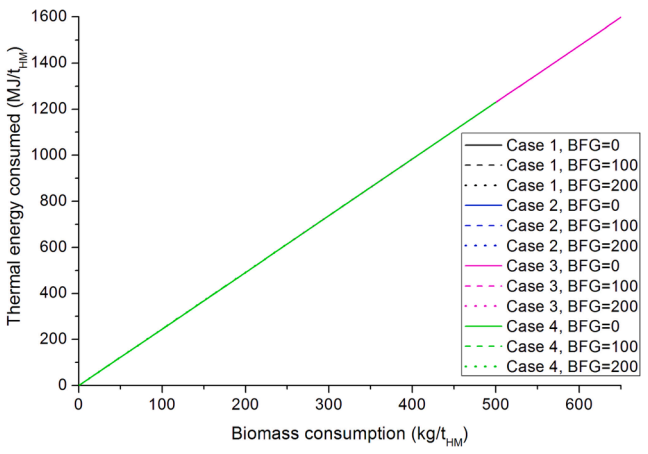

Fig. 17. Thermal energy consumed (KPI11) vs. biomass consumption in pyrolysis (Table 1) and BFG consumed in methanation, for the novel integration of oxygen blast furnaces with pyrolysis and power to gas (Fig. 3).

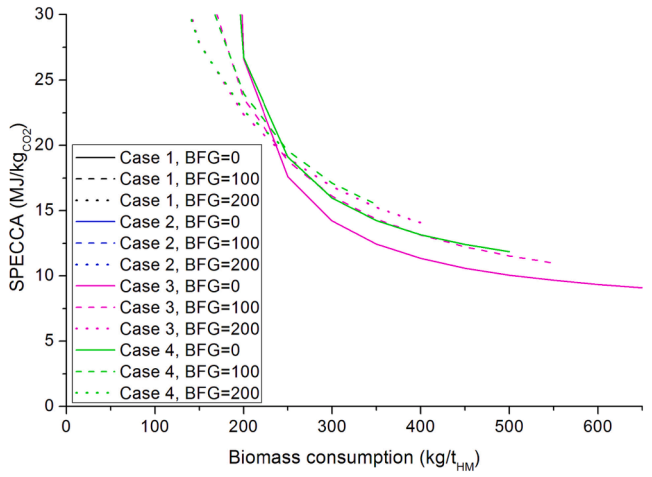

Fig. 18. Specific primary energy consumption per unit of CO_2 avoided (KPI12) vs. biomass consumption in pyrolysis (Table 1) and BFG consumed in methanation, for the novel integration of oxygen blast furnaces with pyrolysis and power to gas (Fig. 3).

Cross-referencing these results with the corresponding CO_2 avoidance, we can calculate the SPECCA (Specific Primary Energy Consumption per unit of CO_2 avoided). As illustrated earlier (Fig. 15), there is a significant CO_2 avoidance only for Case 3 and 4, at biomass consumptions above 200 kg/t_{HM}. This explains why reasonable values for the SPECCA are only observed in these situations, as depicted in Fig. 18. The SPECCA rapidly decreases up to biomass consumptions of 250 kg/t_{HM}, after which the drop rate slows down. This occurs because the amount of CO_2 avoided appears in the denominator of Eq.(5), and it diverges as the denominator approaches 0. Considering the limitation of a 2000 °C flame temperature, the lower SPECCA for Case 3 is 9.8 MJ/kg_{CO2}, and for Case 4 is 13 MJ/kg_{CO2}, with no BFG sent to methanation (no carbon recycling).

To identify the optimal configuration among all the case studies, we depict net CO_2 emissions against energy consumption at the technical limit of a 2000 °C flame temperature (Fig. 19). As elucidated in the discussion of the KPI, only Case 3 and Case 4 result in substantial CO_2 reductions compared to conventional air-blown blast furnaces. For these two cases, prioritizing increased biomass consumption over BFG consumption leads to lower energy consumptions and greater CO_2 abatements. The most favorable configuration is Case 3 (pyrolysis at 700 °C) with no BFG sent to methanation, yielding 559 kg/t_{HM} net CO_2 emissions while consuming 7,612 MJ/t_{HM}.

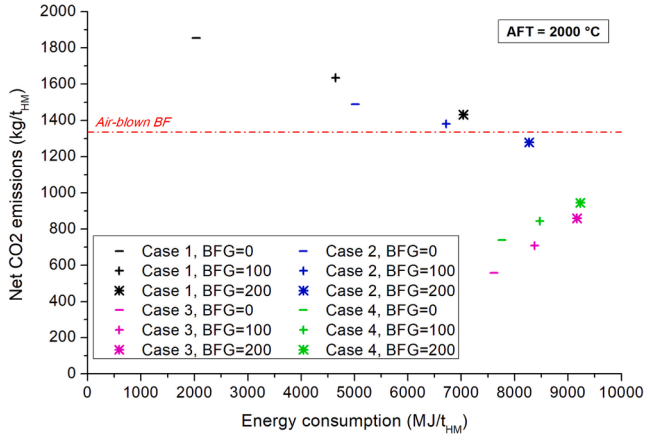

Fig. 19. Net CO_2 emissions (KPI09) vs. energy consumption (KPI10 + KPI11), for the novel integration of oxygen blast furnaces with pyrolysis and power to gas (Fig. 3). Each case is plotted at the maximum biomass consumption, i.e., at the technical limit of 2000 °C flame temperature.

5. Discussion on benchmarking

After an analysis of the novel proposal that integrates oxygen blast furnaces, biomass pyrolysis, and methanation, it has been determined that optimal performance is achieved when pyrolysis is set at 700 °C, and no BFG is directed to methanation. Subsequently, we compare this integration with other OBFs found in the literature, using categories such as CO_2 abatement, Low investment, Efficiency, Downstream self-sufficiency, and Low fossil dependence. These categories are scaled on a 0 – 1 range, utilizing data from Table 5, and are presented in radar plots (Fig. 20). CO_2 abatement is tied to the amount of CO_2 avoided, ranging from a minimum of 0 kg/t_{HM} to a maximum of 1336 kg/t_{HM}, which corresponds to the emissions of a conventional air-blown blast furnace. The Low investment category is linked to the required electrolysis power capacity, with 0 in this category corresponding to the highest capacity required and 1 corresponding to the lowest (i.e., the lowest investment). Efficiency is directly derived from SPECCA, with the radar plot's 0 – 1 range equivalent to 17.8 – 0.0 MJ/kg_{CO2}. Downstream self-sufficiency indicates the availability of BFG for downstream processes, with the 0 – 1 range in this category equaling 0 – 6,730 MJ/t_{HM}, the highest value found during benchmarking. Lastly, Low fossil dependence provides an idea of the total fossil fuel consumed. A Low fossil dependence of 1 corresponds to no fossil fuel consumption, while a Low fossil dependence of 0 corresponds to 488 kg/t_{HM}, the consumption of the conventional air-blown blast furnace.

These categories are defined in a manner that the optimal integration would achieve a score of 1 in each category, streamlining the visualization and comparison of radar plots for the reader. The radar plots clearly illustrate how the conventional air-blown blast furnace excels in low investment, efficiency, and self-sufficiency, given its well-established technology. Naturally, its performance in fossil dependence and CO_2 abatement is inferior when compared to any alternative (Fig. 20). Oxygen blast furnace integrations from the literature utilizing top gas recycling at the tuyeres tend to have lower average investment requirements (0.6 – 0.8 score), maintaining a favorable balance across the remaining categories (0.3 – 0.5 score). Generally, OBF integrations from the literature incorporating top gas recycling at the upper zone exhibit greater self-sufficiency for downstream processes (0.6 – 0.9 score) but lower efficiencies (0 – 0.3 score). In contrast, the novel proposal showcases a notable improvement over any integration previously studied in the literature, excelling in every category. It achieves even higher self-sufficiency than the conventional air-blown blast furnace (without accounting for electrolysis consumption, scoring 1.0), and solid scores (0.5 – 0.6) in every other aspect. Consequently, the integration of biomass charcoal and oxygen blast furnaces may result in superior CO_2 reductions with lower energy penalties than comparable alternatives.

Table 5
Comparison of the performance of the novel proposal with all the OBF integrations found in literature, and with conventional air-blown blast furnaces.

	Net CO_2 emissions (kg/t_{HM})	Electrolysis power ($MW/(t_{HM}/h)$)	SPECCA (MJ/kg_{CO2})	Fossil fuel (kg/t_{HM})	BFG available downstream (MJ/t_{HM})	Ref.
Air-blown blast furnace • Pulverized coal at tuyeres	1336	–	–	488	5084	[33]
Oxygen blast furnace • TGR at tuyeres • SNG (from pure CO_2) at tuyeres	925	1.50	17.8	345	3566	[25]
Oxygen blast furnace • TGR at tuyeres • SNG (from sweet gas) at tuyeres	925	0.98	10.1	351	2239	[25]
Oxygen blast furnace • TGR at tuyeres • SNG (from BFG) at tuyeres	910	1.18	12.5	350	2740	[25]
Oxygen blast furnace • TGR at tuyeres • H_2 at tuyeres	905	1.22	13.6	346	3451	[25]
Oxygen blast furnace • TGR at preparation zone • SNG (from pure CO_2) at tuyeres	738	3.96	17.5	279	4470	[30]
Oxygen blast furnace • TGR at preparation zone • SNG (from BFG) at tuyeres	747	3.03	13.8	280	3966	[31]
Oxygen blast furnace • TGR at preparation zone • H_2 at tuyeres	833	2.90	14.0	307	6147	[31]
Oxygen blast furnace • TGR at tuyeres and preparation zone • SNG (from pure CO_2) at tuyeres	811	2.32	12.0	300	1143	[32]
Oxygen blast furnace • TGR at preparation zone • SNG (from pyrolysis syngas) at tuyeres • Charcoal at tuyeres	559	1.68	9.8	223	6730	This study

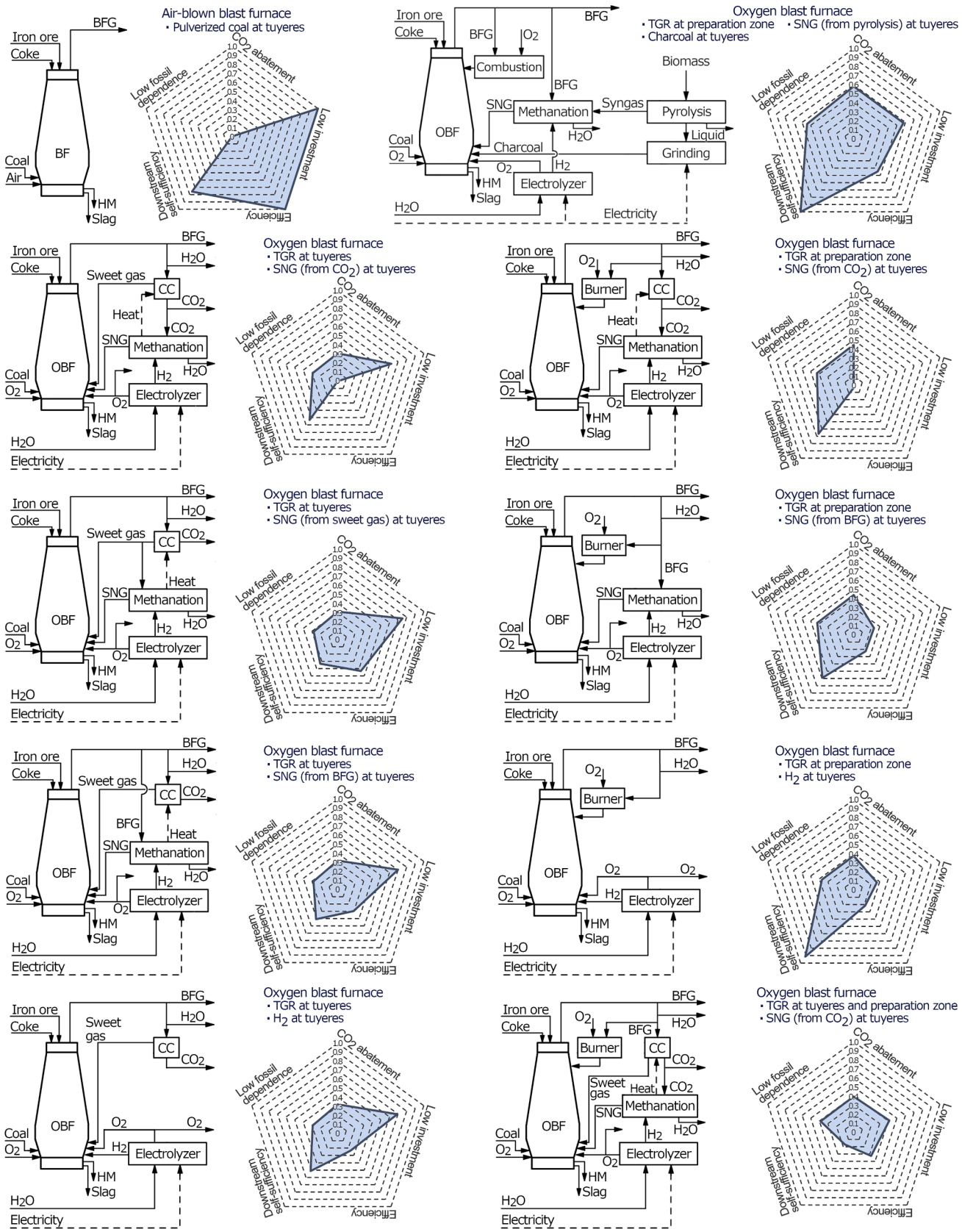

Fig. 20. Radar plot comparing the conventional air-blown blast furnace, the novel proposal, and the eight oxygen blast furnaces integrations found in literature. Categories are explained in the text.

6. Conclusions

This paper introduces an innovative approach to mitigate CO_2 emissions in blast furnaces. The proposed method involves a combination of top gas recycling in the upper zone, an oxy-fuel regime, power to gas technology, and biomass pyrolysis (see Fig. 3). The study encompasses different case scenarios, wherein the temperature of pyrolysis is changed (300 °C, 500 °C, 700 °C, and 900 °C), and the quantity of blast furnace gas directed to methanation for carbon recycling is varied. Pinus radiata waste, readily available at a large scale and low cost in Chile and Spain, was selected as the biomass for this analysis.

The innovative proposal underwent assessment through the extended operating line methodology, which was implemented in Aspen Plus. It is important to note that this model has been previously validated in other studies. All simulations are presented here for the first time, accessible in open access as supplementary material accompanying this paper. The characterization is grounded in 12 key performance indicators, encompassing factors such as flame temperature, coke consumption, net CO_2 emissions, and SPECCA.

To ensure that the flame temperature remains above 2000 °C, the maximum biomass consumption for a 500 t_{HM}/h blast furnace should range between 0.34 and 2.23 Mt/y. This variation depends on the pyrolysis temperature and the quantity of BFG methanized. Considering this technical constraint, the consumption of renewable fuel in the blast furnace falls between 114 and 273 kg/t_{HM} (charcoal plus SNG), allowing for a reduction in coke consumption. When the pyrolysis temperature is set at 300 °C or 500 °C, coke consumption decreases more rapidly with the recycling of BFG through methanation. On the contrary, if the pyrolysis temperature is 700 °C or 900 °C, it is more efficient to use charcoal to decrease coke requirements and consequently reduce CO_2 emissions. Indeed, only utilizing pyrolysis at 700 °C – 900 °C leads to actual CO_2 savings compared to conventional air-blown furnaces. Nevertheless, high-temperature pyrolysis may yield substantial CO_2 reductions of up to 58% without the need for geological storage, surpassing any other OBF concept found in the literature. Furthermore, the lowest SPECCA is 9.8 MJ/kg_{CO2}, corresponding to the case that achieves the maximum CO_2 avoidance. This is accomplished with the novel proposal operating the pyrolysis at 700 °C and without recycling BFG through methanation.

When incorporating the optimal configuration of the novel proposal into a benchmarking analysis, it emerges as superior in every category compared to any other oxygen blast furnace integration found in the literature. The CO_2 reduction is notably higher, surpassing the second-best alternative by 13 percentage points. The required electrolysis capacity, a significant driver of capital expenditure, is 57% lower than that of the alternative with the highest CO_2 reduction. Additionally, the specific primary energy consumption per unit of CO_2 avoided is 3% lower than the alternative with the lowest SPECCA and 44% lower than the alternative with the highest CO_2 reduction. Furthermore, the novel proposal yields more energy in the form of blast furnace gas for downstream processes compared to the conventional air-blown blast furnace. Given these compelling factors, the integration of biomass pyrolysis with oxygen blast furnaces should be prioritized whenever feasible.

The outcomes of this study are constrained by the employed methodology (extended operating line), fundamentally reliant on energy and mass balances along the blast furnace. More intricate simulations would offer enhanced insights into the impact of introducing biochar through the tuyeres. Additionally, it is imperative to conduct experimental research to substantiate these simulations, particularly focusing on characterizing the combustion of biochar at the tuyeres. This is crucial to ensure that the reactivity and burnout align with those observed for pulverized coal.

Declaration of competing interest

The authors declare that they have no known competing financial interests or personal relationships that could have appeared to influence the work reported in this paper.

Data availability

No data was used for the research described in the article.

Acknowledgments

This project has received funding from the European Union's Framework Programme for Research and Innovation Horizon 2020 (2014-2020) under the Marie Skłodowska-Curie Grant Agreement No. 887077. The author M.B. acknowledges the R&D project TED2021-130000B-I00, funded by MCIN/AEI/10.13039/501100011033 and by the "European Union NextGenerationEU/PRTR".

Appendix A. Supplementary data

Supplementary data to this article can be found online at https://doi.org/10.1016/j.enconman.2023.117916.

References

[1] International Energy Agency, Iron and Steel Technology Roadmap. 2020.
[2] Midrex Technologies, 2022. The Midrex (R) Process. n.d.
[3] Bene C, Mahmoud M, Opinska LG, Rademaekers K. Moving Towards Zero-Emission Steel 2021:46.
[4] Perpiñán J, Peña B, Bailera M, Eveloy V, Kannan P, Raj A, et al. Integration of carbon capture technologies in blast furnace based steel making: A comprehensive and systematic review. Fuel 2023;336:127074. https://doi.org/10.1016/j.fuel.2022.127074.
[5] von Scheele J. Decarbonization of Ironmaking. MM Steel Club 2021.
[6] Sato M, Takahashi K, Nouchi T, Ariyama T. Predictcion of next-generation ironmaking process based on oxygen blast furnace suitable for CO2 mitigation and energy flexibility. ISIJ Int 2015;55:2105–14. https://doi.org/10.2355/isijinternational.ISIJINT-2015-264.
[7] Quader MA, Ahmed S, Raja Ghazilla RA, Ahmed S, Dahari M. Evaluation of criteria for CO2 capture and storage in the iron and steel industry using the 2-tuple DEMATEL technique. J Clean Prod 2016;120:207–20. https://doi.org/10.1016/j.jclepro.2015.10.056.
[8] Ho MT, Bustamante A, Wiley DE. Comparison of CO2 capture economics for iron and steel mills. Int J Greenh Gas Control 2013;19:145–59. https://doi.org/10.1016/j.ijggc.2013.08.003.
[9] Jin P, Jiang Z, Bao C, Lu Y, Zhang J, Zhang X. Mathematical Modeling of the Energy Consumption and Carbon Emission for the Oxygen Blast Furnace with Top Gas Recycling. Steel Res Int 2016;87:320–9. https://doi.org/10.1002/srin.201500054.
[10] Helle H, Helle M, Pettersson F, Saxén H. Multi-objective Optimization of Ironmaking in the Blast Furnace with Top Gas Recycling. ISIJ Int 2010;50:1380–7. https://doi.org/10.2355/isijinternational.50.1380.
[11] Helle H, Helle M, Saxén H, Pettersson F. Optimization of Top Gas Recycling Conditions under High Oxygen Enrichment in the Blast Furnace. ISIJ Int 2010;50:931–8. https://doi.org/10.2355/isijinternational.50.931.
[12] Zhang W, Zhang J, Xue Z, Zou Z, Qi Y. Unsteady Analyses of the Top Gas Recycling Oxygen Blast Furnace. ISIJ Int 2016;56:1358–67. https://doi.org/10.2355/isijinternational.ISIJINT-2016-090.
[13] Ariyama T, Sato M, Nouchi T, Takahashi K. Evolution of blast furnace process toward reductant flexibility and carbon dioxide mitigation in steel works. ISIJ Int 2016;56:1681–96. https://doi.org/10.2355/isijinternational.ISIJINT-2016-210.
[14] She X, An X, Wang J, Xue Q, Kong L. Numerical analysis of carbon saving potential in a top gas recycling oxygen blast furnace. J Iron Steel Res Int 2017;24:608–16. https://doi.org/10.1016/S1006-706X(17)30092-4.
[15] Zhang W, Xue Z, Zhang J, Wang W, Cheng C, Zou Z. Medium oxygen enriched blast furnace with top gas recycling strategy. J Iron Steel Res Int 2017;24:778–86. https://doi.org/10.1016/S1006-706X(17)30117-6.
[16] Arasto A, Tsupari E, Kärki J, Lilja J, Sihvonen M. Oxygen blast furnace with CO2 capture and storage at an integrated steel mill-Part I: Technical concept analysis. Int J Greenh Gas Control 2014;30:140–7. https://doi.org/10.1016/j.ijggc.2014.09.004.
[17] Jin P, Jiang Z, Bao C, Hao S, Zhang X. The energy consumption and carbon emission of the integrated steel mill with oxygen blast furnace. Resour Conserv Recycl 2017;117:58–65. https://doi.org/10.1016/j.resconrec.2015.07.008.
[18] Murai R, Sato M, Ariyama T. Design of Innovative Blast Furnace for Minimizing CO2 Emission Based on Optimization of Solid Fuel Injection and Top Gas Recycling. ISIJ Int 2004;44:2168–77. https://doi.org/10.2355/isijinternational.44.2168.
[19] Wang H, Chu M, Guo T, Zhao W, Feng C, Liu Z, et al. Mathematical Simulation on Blast Furnace Operation of Coke Oven Gas Injection in Combination with Top Gas

Recycling. Steel Res Int 2016;87:539–49. https://doi.org/10.1002/srin.201500372.
[20] Helle M, Saxén H. Operation windows of the oxygen blast furnace with top gas recycling. ISIJ Int 2015;55:2047–55. https://doi.org/10.2355/isijinternational.ISIJINT-2015-083.
[21] Bailera M, Nakagaki T, Kataoka R. Revisiting the Rist diagram for predicting operating conditions in blast furnaces with multiple injections. Open Res Eur 2021;1. 10.12688/openreseurope.14275.1.
[22] Bargiacchi E, Candelaresi D, Valente A, Spazzafumo G, Frigo S. Life Cycle Assessment of Substitute Natural Gas production from biomass and electrolytic hydrogen. Int J Hydrogen Energy 2021;46:35974–84. https://doi.org/10.1016/j.ijhydene.2021.01.033.
[23] Faria DG, Carvalho MMO, Neto MRV, de Paula EC, Cardoso M, Vakkilainen EK. Integrating oxy-fuel combustion and power-to-gas in the cement industry: A process modeling and simulation study. Int J Greenh Gas Control 2022;114:103602. https://doi.org/10.1016/j.ijggc.2022.103602.
[24] Perpiñán J, Bailera M, Romeo LM, Peña B, Eveloy V. CO2 Recycling in the Iron and Steel Industry via Power-to-Gas and Oxy-Fuel Combustion. Energies 2021;14:7090. https://doi.org/10.3390/en14217090.
[25] Bailera M, Nakagaki T, Kataoka R. Limits on the integration of power to gas with blast furnace ironmaking. J Clean Prod 2022;134038. https://doi.org/10.1016/J.JCLEPRO.2022.134038.
[26] Tseitlin MA, Lazutkin SE, Styopin GM. A Flow-chart for Iron Making on the Basis of 100% Usage of Process Oxygen and Hot Reducing Gases Injection. ISIJ Int 1994;34:570–3. https://doi.org/10.2355/isijinternational.34.570.
[27] Zhou Z, Yi Q, Wang R, Wang G, Ma C. Numerical Investigation on Coal Combustion in Ultralow CO2 Blast Furnace: Effect of Oxygen Temperature. Processes 2020;8:877. https://doi.org/10.3390/pr8070877.
[28] Takahashi K, Nouchi T, Sato M, Ariyama T. Perspective on Progressive Development of Oxygen Blast Furnace for Energy Saving. ISIJ Int 2015;55:1866–75. https://doi.org/10.2355/isijinternational.ISIJINT-2015-196.
[29] Liu Y, Shen Y. Modelling and optimisation of biomass injection in ironmaking blast furnaces. Prog Energy Combust Sci 2021;87:100952. https://doi.org/10.1016/j.pecs.2021.100952.
[30] Perpiñán J, Bailera M, Peña B, Romeo LM, Eveloy V. High oxygen and SNG injection in blast furnace steelmaking with Power to Gas integration and CO2 recycling 2023.
[31] Perpiñán J, Bailera M, Peña B, Eveloy V, Romeo LM. Full oxygen blast furnace steelmaking: direct H2 injection or methanized BFG injection 2023.
[32] Perpiñán J, Bailera M, Peña B, Kannan P, Eveloy V, Romeo LM. Power to Gas and Top Gas Recycling integration in an oxygen blast furnace steelmaking industry 2023.
[33] Bailera M. Comparing different syngas for blast furnace ironmaking by using the extended operating line methodology. Fuel 2023;333:126533. https://doi.org/10.1016/j.fuel.2022.126533.
[34] Spichiger JB, Verdugo EM. Potencial de Biomasa Forestal: Potencial de generación de energía por residuos del manejo forestal en Chile. 2008.
[35] Antonio GJ. Study of wood chip production from forest residues in Chile. Biomass 1984;5:167–79. https://doi.org/10.1016/0144-4565(84)90021-0.
[36] CONAF. Superficies de uso de suelo regional. 2021.
[37] Solar J, Caballero BM, López-Urionabarrenechea A, Acha E, Arias PL. Pyrolysis of Forestry Waste in a Screw Reactor with Four Sequential Heating Zones: Influence of Isothermal and Nonisothermal Profiles. Ind Eng Chem Res 2021;60:18627–39. https://doi.org/10.1021/acs.iecr.1c01932.
[38] Solar J, Caballero B, De Marco I, López-Urionabarrenechea A, Gastelu N. Optimization of Charcoal Production Process from Woody Biomass Waste: Effect of Ni-Containing Catalysts on Pyrolysis Vapors. Catalysts 2018;8:191. https://doi.org/10.3390/catal8050191.
[39] Solar J, Caballero BM, Barriocanal C, Lopez-Urionabarrenechea A, Acha E. Impact of the Addition of Pyrolysed Forestry Waste to the Coking Process on the Resulting Green Biocoke. Metals (Basel) 2021;11:613. https://doi.org/10.3390/met11040613.
[40] Solar J, de Marco I, Caballero BM, Lopez-Urionabarrenechea A, Rodriguez N, Agirre I, et al. Influence of temperature and residence time in the pyrolysis of woody biomass waste in a continuous screw reactor. Biomass Bioenergy 2016;95:416–23. https://doi.org/10.1016/j.biombioe.2016.07.004.
[41] Bailera M, Nakagaki T, Kataoka R. Extending the Operating Line Methodology to Consider Shaft and Preheating Injections in Blast Furnaces. ISIJ Int 2022:ISIJINT-2022-111. 10.2355/isijinternational.ISIJINT-2022-111.
[42] Babich A, Senk D, Solar J, de Marco I. Efficiency of biomass use for blast furnace injection. ISIJ Int 2019;59:2212–9. https://doi.org/10.2355/isijinternational.ISIJINT-2019-337.
[43] Bailera M, Nakagaki T, Kataoka R. Extending the operating line methodology to consider shaft and preheating injections in blast furnaces. ISIJ Int 2022:62. https://doi.org/10.2355/isijinternational.ISIJINT-2022-111.
[44] Rist A, Meysson N. A dual graphic representation of the blast-furnace mass and heat balances. JOM 1967;19:50–9. https://doi.org/10.1007/bf03378564.
[45] Izumiya K, Shimada I. Methane producing technology from CO2 for carbon recycling. In: The First Symposium on Carbon Ultimate Utilization Technologies for the Global Environment. CUUTE-1; 2021. p. 34–5.
[46] Geerdes M, Chaigneau R, Lingiardi O. Molenaar R van O, R. SY: Warren J. Modern Blast Furnace Ironmaking An Introduction. IOS Press; 2020.
[47] NEL Hydrogen. M Series Containerized Proton Exchange Membrane (PEM) Hydrogen Generation Systems 2021. https://nelhydrogen.com/wp-content/uploads/2022/06/M-Series-Containerized-Spec-Sheet-Rev-E.pdf (accessed September 5, 2022).
[48] Perpiñán J, Bailera M, Peña B, Romeo LM, Eveloy V. Technical and economic assessment of iron and steelmaking decarbonisation via power to gas and amine scrubbing. Energy 2023.
[49] Crombie K. Investigating the potential for a self-sustaining slow pyrolysis system under varying operating conditions 2014;162:148–56. https://doi.org/10.1016/j.biortech.2014.03.134.